# CHARACTERISTICS OF A PARAMETRIC SYNCHRONOUS MOTOR AND A PARAMETRIC INDUCTION GENERATOR MADE FOR TEST

S. Kikuchi, Y. Sakamoto* and K. Murakami*

Abstract-This paper describes the structure and the operation of two new machines using rotational field based on a parametric oscillation. One of the machines is the parametric synchronous motor using permanent magnet rotor. Another one is the parametric induction generator.

These machines have a number of interesting features in construction and operation. The results of this study seem to be useful for development of electrical machines and to introduce a new field for application of the parametric machine in the future.

## INTRODUCTION

The parametric induction motor utilizing a parametric oscillation which is induced by using two C-cores was reported by the authors [1] and the various characteristics have been examined from different point of view. [2][3] The motor has superior advantages as compared with ordinary motor in construction. For example, the structure is very simple because of slotless stator and the windings of the motor can be pre-wound together with C-shape magnetic cores. Utilizing the simplicity in structure, we made two new parametric machines. One of the machines is a parametric synchronous motor using permanent magnet rotor. Another one is the parametric induction generator. By using the test machines, we carried out the experiments and obtained good results. In this paper we describe these results.

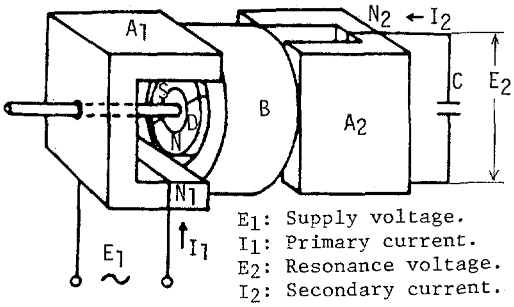


Fig. 1. Outline of a parametric synchronous motor.

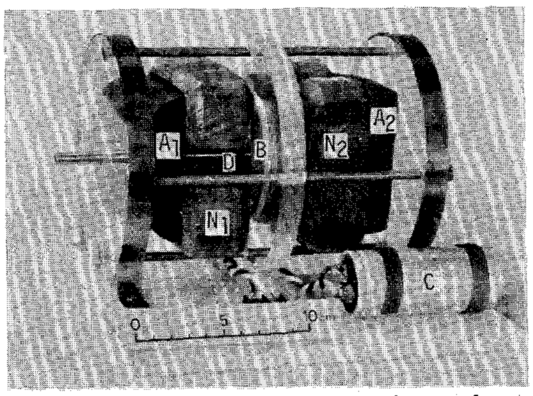


Fig. 2. General view of the parametric synchronous motor.

Manuscript received March 2, 1984

With Department of Electrical Engineering, Tohoku Gakuin University, Tagajo, Japan 985

*With Department of Electrical Engineering, Tohoku University, Sendai, Japan 980

## STRUCTURE AND CHARACTERISTICS

(1) Parametric synchronous motor

Figure 1 shows the outline of a parametric synchronous motor proposed by the authors. In the figure, $A_1$ and $A_2$, which consist of C-shape cores, are the magnetic circuit for excitation. These cores are 90 degrees relative to each other in space. B is a common magnetic circuit for generating a rotating field. $N_1$ and $N_2$ are windings wound around the magnetic circuit $A_1$ and $A_2$, respectively. C is a resonance capacitor used for parametric oscillation. D is a non-salient pole type rotor.

Figure 2 shows a general view of a parametric synchronous motor built for experiments. We used the commercial cut cores as the magnetic circuit $A_1$, $A_2$ for excitation and the Fe-Si plates (0.35 mm thickness) as the common magnetic circuit B. A slit was provided in the common magnetic circuit in order to increase the output power.[2]

The rotor is a non-salient pole type with a permanent magnet made of commercial strontium ferrite. The composition and the properties of the permanent magnet are shown in Table 1. The structure and dimensions of the rotor are shown in Fig. 3. We used an external driving motor to start the parametric synchronous motor in experiments, although self-starting motor will be used in practically by using the rotor with amortisseur winding.

Table 1. Composition and properties of strontium ferrite permanent magnet.

| | |
|---|---|
| Compositions | $SrO \cdot 6Fe_2O_3$ |
| Residual Flux Density ($B_r$) | 0.42 (T) |
| Intrinsic Coercive Force ($IH_c$) | 239 (kA/m) |
| Coercive Force ($BH_c$) | 235 (kA/m) |

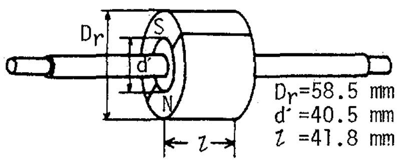


Fig. 3. Structure and dimensions of the rotor.

Figure 4 shows an example of the load characteristics of the parametric synchronous motor built for experiments. The output power P is obtained by the following equations.

$$P=2\pi N_s T/60 \quad \text{(W)} \tag{1}$$

$$N_s=120 \cdot f/p \quad \text{(rpm)} \tag{2}$$

where $N_s$ is the synchronous speed, f is the supply frequency, p is the number of poles and T(N.m) is the torque. It reveals that the efficiency $\eta$ increases as the output power P increases and that the maximum efficiency $\eta_m$ is the value of 62.5 % at the output power P=106 W. It seems that this value is available for practical uses. On the other hand, the resonance voltage $E_2$ decreases with the output power P increasing. When the output power P exceeds a certain value, $E_2$ decreases rapidly, then the parametric oscillation stops and the synchronous motor pull-out torque is exceeded.

0018-9464/84/0900-1792$01.00©1984 IEEE

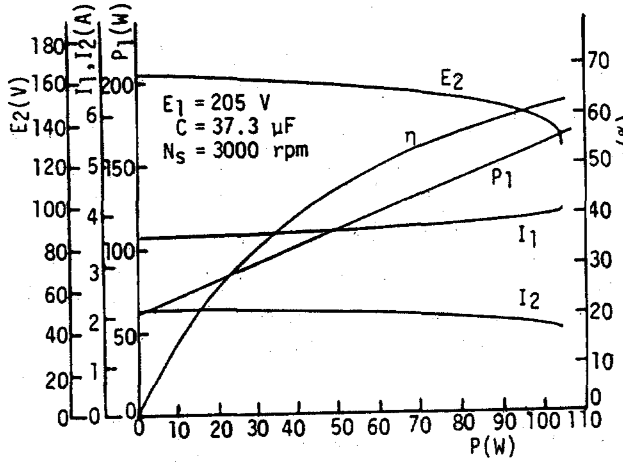


Fig. 4. Load characteristics of the parametric synchronous motor. $P_1$: Input power.

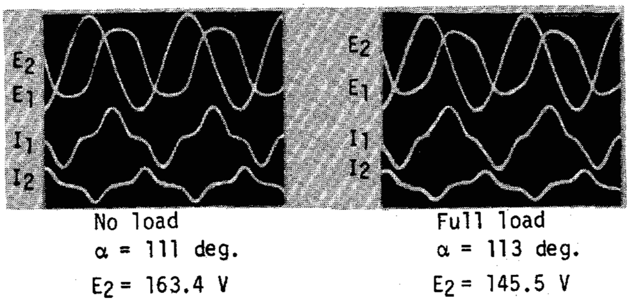


**Fig. 5. Voltage and current waveforms of each part when the motor operates at no load and full load condition.**

Figure 5 shows the voltage and the current waveforms of each part when the motor operated at no load and load condition. It reveals that the phase difference $\alpha$ between $E_1$ and $E_2$ increases and the value of the resonance voltage $E_2$ decreases as the output power P increases.

Next, we have measured the gap flux in order to examine how the rotor flux influences the performance characteristics of the motor. The gap flux was measured by using 24 search coils attached inside a common magnetic circuit.

Figure 6 shows the position of the search coils along the circumference of the common magnetic circuit. The search coils were attached in 3 lines along the direction of the rotor length.

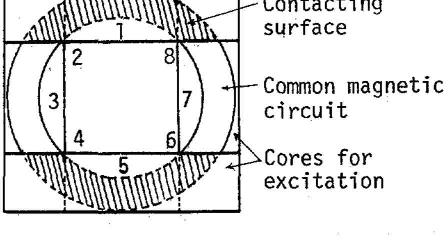


Fig. 6. Position of the search coils.

Figure 7 shows the torque T versus the load angle $\delta$ curve measured under the same condition in Fig. 5. The figure reveals that the torque increases almost linearly in the region of load angle $\delta \leqq \pi/4$, although the torque T is proportional to $\sin\delta$. And then the parametric synchronous motor becomes pull-out condition at $\delta \cong \pi/2$.

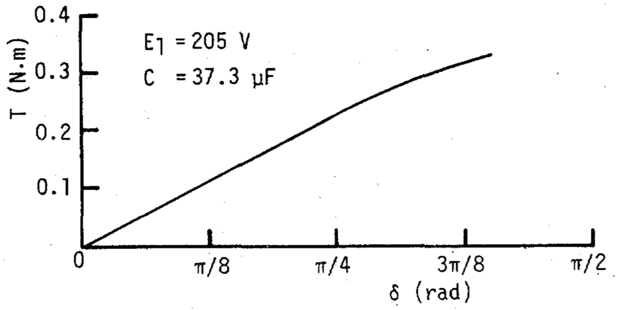


Fig. 7. Torque versus the load angle curve.

Figure 8 shows the gap flux distribution along the circumference at the central part of the common magnetic circuit. In the figure, the line indicates the measured values when the motor operated at full load condition and the dotted line indicates the values at no load condition. It reveals that the gap flux increases at search coil positions 2, 6 under the full load condition.

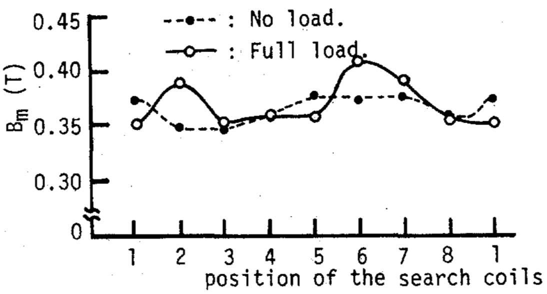


**Fig. 8. Gap flux distribution along the circumference at the central part of the common magnetic circuit.**

Figure 9 shows the gap flux waveform measured when the motor operated under no exciting condition. In this case the gap flux is produced only by the permanent magnet of the rotor. The figure reveals that the waveform includes high frequency components and that the gap flux is a almost rectangular distribution.

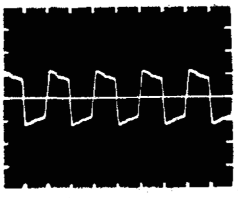

**Fig. 9. Gap flux waveform.**

Figure 10 shows the relation between the output power P and the mean gap flux density $\overline{B_m}$. $\overline{B_m}$ indicates the mean value of the flux density measured by using 24 search coils. This figure reveals that the mean flux density $\overline{B_m}$ remains constant as the output power P increases.

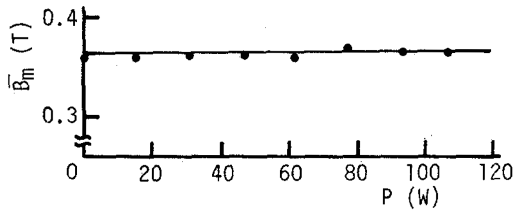


Fig. 10. Relation between the output power P and the mean flux density $\bar{B}_m$.

As shown in Fig. 8 and 10, it was clear that the rotor flux is very large as compared with the flux induced by the primary current I and that only the gap flux distribution varies with the output power P increasing.

(2) Parametric induction generator

When a rotor of induction motor is rotated at the velocity over synchronous speed by an external driving motor, the induction motor operates as an induction generator. Based on this operating principle, we discussed the behavior of a parametric induction generator. We used a parametric induction motor with cage-rotor shown in Fig. 11.

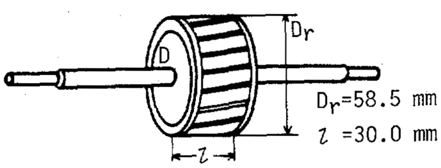


Fig. 11. Cage-rotor.

Figure 12 shows an example of the load characteristics of the parametric induction generator. In the figure, it reveals that this motor operates as an induction generator when the slip s=-0.06. In this case, the output power $P_{1g}$ has a maximum when the slip s=-0.21 and the maximum value $P_{max}$ is equal to 33 W. The efficiency $\eta_g$ of the induction generator is obtained as follows:

$$\eta_g = (P_{1g}/P_r) \times 100 \quad (\%) \qquad (3)$$

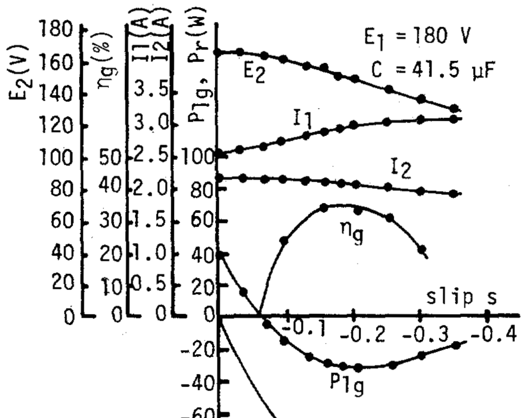


Fig. 12. Load characteristics of the parametric induction generator.

where $P_{1g}$ is the output power and $P_r$ is the input power of the external driving motor.

As shown in Fig. 12, the efficiency $\eta_g$ has maximum at the slip s=-0.16 and the maximum value is $\eta_{gmax}$=33 %.

Figure 13 shows the voltage and the current waveforms of primary and secondary parts of the generator when it operated at the slip s=-0.21.

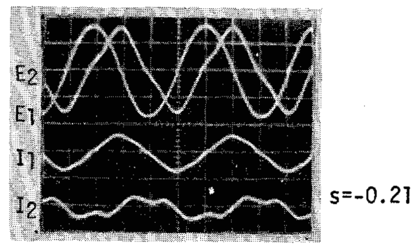


Fig. 13. Voltage and current waveforms.

Figure 14 shows the supply voltage dependence of output power $P_{1g}$ and efficiency $\eta_g$ for various values of the resonance capacitor. The figure reveals that the efficiency $\eta_g$ has a maximum at the supply voltage $E_1$=150 V regardless of the value of resonance capacitor C although the maximum output power $P_{1gmax}$ increases with the value of resonance capacitor C increasing. The high efficiency can be obtained, when the machine is optimum designed.

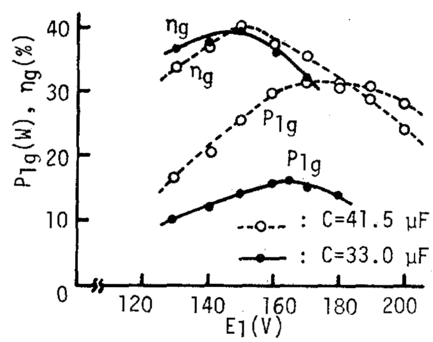


Fig. 14. Supply voltage dependance of the output power and the efficiency.

## CONCLUSION

Two new parametric machines have been proposed and built by the authors. We can confirm that various AC machines are able to be manufactured by utilizing a parametric oscillation. The results of this study seem to be useful for development of electrical machines and to introduce a new field for application of the parametric machine in the future.

## REFERENCES

[1] K. Murakami, S. Kikuchi and T. Watanabe, "Characteristics of a new AC motor making good use of parametric oscillation", IEEE Trans. Magn., vol. MAG-16, pp.931-933, Sept. 1980.
[2] S.Kikuchi, Y.Sakamoto, O.Ichinokura and K.Murakami, "An interesting method for obtaining parametric motors with excellent performance", IEEE Trans. Magn., vol. MAG-18, pp.1746-1748, Nov. 1982.
[3] K.Murakami, S.Kikuchi, T.Watanabe and H.Miyazaki, "Characteristics of two new parametric motors for high speed rotation and disk rotation", IEEE Trans. Magn., vol. MAG-18, pp.1743-1745, Nov. 1982.